JOURNAL OF MATERIALS SCIENCE 23 (1988) 2505–2511

A revision of the double-torsion technique for brittle materials

OSAM SANO
Faculty of Engineering, Yamaguchi University Ube 755, Japan

Serious doubts about the constant-K characteristics of double-torsion specimens have been expressed in recent years. However, compliance calibration shows that the energy release rate and hence the stress intensity factor are independent of the crack length in this technique. Relatively large scattering in the results obtained by the load-relaxation method makes the data unreliable. The load-relaxation experiments should be carried out in combination with other methods. A theoretical calculation of the load–deformation curve under a constant displacement rate gives a rough estimation of the stress corrosion index. The subcritical crack growth data can be given, in principle, by only one experimental run of the constant displacement rate method of double-torsion testing.

1. Introduction

Subcritical crack growth can be observed for various brittle materials such as glass [1], ceramics [2] and rocks [3]. The slow crack growth is brought about by stress corrosion which produces weak bond structures because of stress-aided chemical reactions at the point of tensile stress concentration within the material. For silicate materials, the reactive agent is water. Because subcritical crack growth is known as a source of time-dependent fracture of these materials [1–3], information about the subcritical crack growth is very important in the failure prediction of engineering materials and crustal rocks.

Several fracture mechanics tests for investigating subcritical crack growth have been proposed in the past twenty years [4]. Among them, the double-torsion technique should be one of the most useful methods for opaque materials in hostile environments, because of its simple loading system, its simple configuration of the specimen, easy pre-cracking, and independence of the stress intensity factor on crack length. The double-torsion method was introduced by Outwater and Gerry [5] and Kies and Clark [6]. In the original double-torsion test the constant load method was used [6], where the load was kept constant and a deflection of the plate was monitored. The crack velocity can be given, in this method, by the applied load and the deflection rate of the plate.

Evans [7] introduced two other methods, namely the constant displacement rate method and the load-relaxation method. In the former, the displacement rate of the loading point is kept constant. When the load increases up to a critical level, the rate of change in the specimen's compliance due to the crack's advance cancels the increasing rate of load. The load then reaches the maximum level and is held constant. The crack velocity can be determined from the load of the plateau region and the driven rate of the loading point. In the relaxation test, the load is raised rapidly up to a given point and the loading point is fixed. As the crack grows, the compliance of the specimen increases and the load decreases. The crack velocity can be determined from the initial load, the temporal load and the decreasing rate of load. Thus, in the relaxation method the monitoring of only the applied load is required.

As the growth rate V of the crack depends on the stress intensity factor K at the crack-tip and on environmental factors such as temperature and humidity, experimental results are usually collected in stress intensity factor–crack velocity diagrams, namely K–V diagrams. In the two methods, the constant load and the constant displacement rate, only one point in the K–V diagram can be determined by a single experimental run. On the other hand, the relaxation method gives a wide range of data in the K–V diagram, generally from 10^{-10} to 10^{-1} m sec^{-1}, from only a single experimental run. The relaxation method has therefore, been used by many authors [7–13], while the other two methods have been seldom used. A few exceptions are found in Evans and Wiederhorn [14], Waza *et al.* [15], Sano [16], Michalske *et al.* [17] and Costin and Mecholsky [18]. However, using the relaxation method for polycrystalline materials, a hysteresis in the K–V diagram has been reported by Pletka and Wiederhorn [12] and Ferber and Brown [13]. Pletka and Wiederhorn suggested that the stress intensity factor should be dependent on the crack length. Although there is serious doubt about double-torsion testing, such hysteresis has been reported only for the relaxation method. We should have another look at the other two methods in the double-torsion technique.

2. Specimens

Materials used in this study are soda-lime glass, Murata basalt, quartz andesite and Oshima granite. Murata basalt (North-eastern Japan) consists mainly of glassy matrix and fine-grained feldspar whose mean grain length is about 0.1 mm. Quartz andesite

0022–2461/88 $03.00 + .12

(South-western Japan) consists mainly of glassy matrix, fine-grained feldspar and quartz. The mean length of the grains is about 0.1 mm. A petrographic description of Oshima granite (South-western Japan) has been given by Sano *et al.* [19]. The mean grain size of Oshima granite is about 1 mm. They are brittle and hard rocks. The uniaxial compressive strengths, for example, under a constant strain rate of 10^{-5} sec^{-1}, are 380, 300 and 220 MPa for quartz andesite, Murata basalt and Oshima granite, respectively.

3. Experimental procedures

A schematic representation of a double-torsion specimen is shown in Fig. 1, where the notation of the specimen's configuration is also shown. The dimensions of the specimens are roughly $W = 40, L = 100, d = 3$ and $d_n = 2.9$ mm for soda-lime glass, and $d = 1.5$ to 2 and $d_n = 0.5$ to 1.5 mm for other materials. The guide groove cut in the central part of the specimen was set downward in the original double-torsion articles, but was set upward in this study according to Pletka *et al.* [8]. Fig. 2 shows an illustration of the double-torsion apparatus used in this study. A stepping motor drives the micrometer head which can apply the load to the specimen. The frequency range of the pulse generator used for the stepping motor is from 10^{-5} to 10^{4} Hz. The maximum pulse rate of the stepping motor is 3 kHz. The accuracy of the load-cell is 1% of full scale. Deformation of the plate was monitored by two linear variable differential transformers (LVDT) (Schaevitz HCD050). Load and deformation were recorded by a X–Y chart recorder. The load was also monitored by an analogue–digital converter of 12 bit resolution. The maximum sampling rate needed for sampling data and recording on to random access memories of a personal computer is 40 μsec. Acoustic emissions were detected by lead zirconate–lead titanate discs. After amplification of 50 dB, the event rate was monitored by using a discriminator and a counter. A threshold level was 30 mV. The crack velocity was estimated by using the usual equations as suggested by Evans [7] for the constant load and constant displacement rate methods. In the relaxation method, the initial compliance C_0, determined from the load–deformation curve was used instead of $(Ba_0 + D)$, namely

$$V = -C_0 P_0 \left(\frac{dP}{dt}\right) \frac{1}{BP^2}$$

where a_0 is the initial crack length, P is the applied load, P_0 is the initial load, t is the time, and B and D are constants [7].

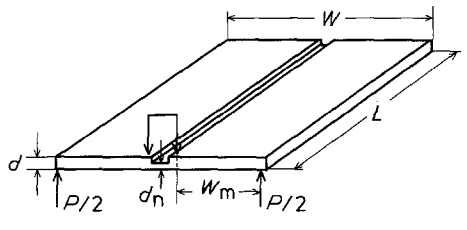

Figure 1 A schematic representation of the double-torsion specimen.

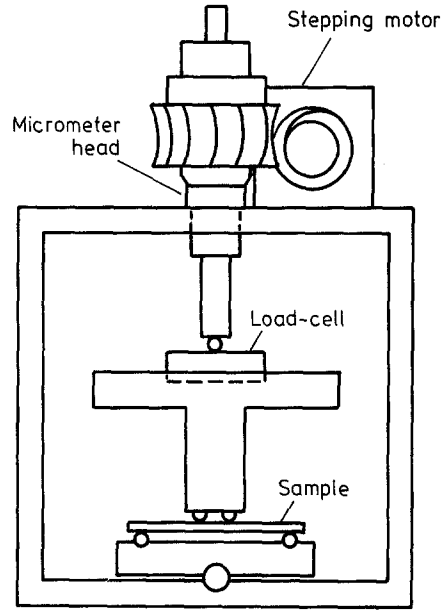

Figure 2 An illustration of the double-torsion apparatus.

4. Experimental results

The hysteresis in the K–V relation observed in several experimental runs of the relaxation test has been pointed out by several authors [12, 13]. Except for glass, the hysteresis was observed for almost all materials used in this study. An example of the hysteresis observed on a GH specimen of Oshima granite is shown in Fig. 3. GH indicates that the crack propagates in a direction normal to the "grain" plane, and that the crack opening direction is normal to the "hardway" plane. These planes are quarryman's terminology for the planes of anisotropy in granites [20], and are characterized by the preferred orientation of the pre-existing cracks [21]. Discordance among the K–V relations of four experimental runs can be seen in Fig. 3. The stress corrosion index, n, for the first to the third run is about 70, but the index from the fourth run is 32. Atkinson and Rawlings [22] found that the stress corrosion index of Westerly granite is 39.1 in air and 34.8 in water, while the

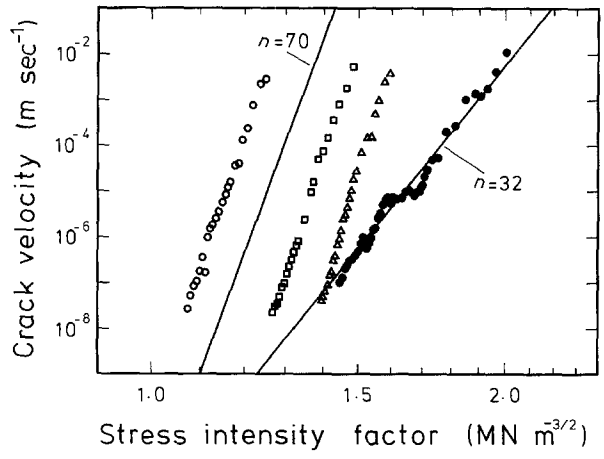

Figure 3 An example of hysteresis in the stress intensity factor–crack velocity diagram observed with GH Oshima granite. Data are plotted on double logarithmic coordinates. GH indicates that the velocity of the crack propagates normal to the grain plane and, simultaneously, opens normal to the hardway plane. (○) 1st test, (□) 2nd test, (△) 3rd test, (●) 4th test.

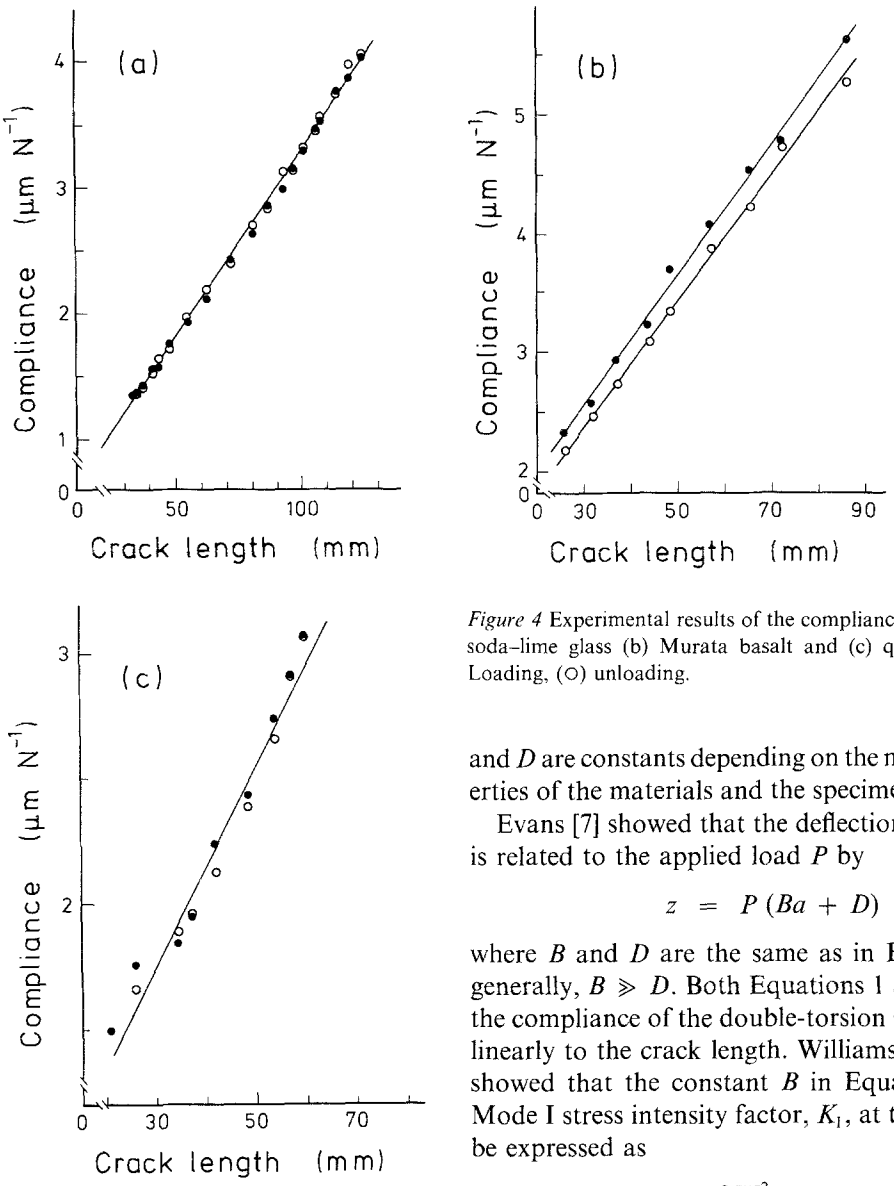

Figure 4 Experimental results of the compliance calibration for (a) soda-lime glass (b) Murata basalt and (c) quartz andesite. (●) Loading, (○) unloading.

author's estimation of the index of the same granite based on Swanson's data [23] is about 57. Although this discrepancy may be due to the anisotropy of Westerly granite, it can also be due to the hysteresis described above. Does the stress intensity factor depend on the crack length, as suggested by Pletka and Wiederhorn [12]?

Compliance calibration tests were carried out for various materials. The applied load was raised slowly to a given level at which the crack should lengthen moderately, and then the load was decreased. The crack length was measured optically, and then the specimen was reloaded again. The compliance of the specimen determined from the load–deformation curve is plotted against the crack length. Fig. 4 shows the results of the compliance calibration tests for soda-lime glass, Murata basalt and quartz andesite. As a relatively large hysteresis was observed for rocks, the compliance was determined for both the loading and unloading parts of the load–deformation curves. The linearity of the compliance against the crack length agrees with what Evans [7] had shown. These relations can be expressed as

$$C = Ba + D \tag{1}$$

where a is the crack length, C is the compliance, and B and D are constants depending on the mechanical properties of the materials and the specimen's dimensions.

Evans [7] showed that the deflection of the plate, z, is related to the applied load P by

$$z = P(Ba + D) \tag{2}$$

where B and D are the same as in Equation 1 and, generally, $B \gg D$. Both Equations 1 and 2 show that the compliance of the double-torsion specimen relates linearly to the crack length. Williams and Evans [24] showed that the constant B in Equation 2 and the Mode I stress intensity factor, K_I, at the crack tip can be expressed as

$$B = \frac{3W_m^2}{Wd^3G} \tag{3}$$

$$K_I = PW_m\left[\frac{3(1+\nu)}{Wd_n d^3}\right]^{1/2} \tag{4}$$

where d, d_n, W and W_m are the same as in Fig. 1. ν and G are the Poisson's ratio and shear modulus of the material, respectively. Using Equation 3, the shear modulus can be determined. The results are shown in Table I with the shear modulus determined by other methods. These moduli are in accordance with each other for the same material, which indicates that Equations 1 to 3 hold well.

When the shape of the curved crack front is constant during the crack advance and f is a numerical constant, the area of the crack surface, A, can be expressed as $A \doteqdot fad_n$. The energy release rate, G, is expressed as [25]

$$G = \frac{P^2}{2}\left(\frac{\partial C}{\partial a}\right)\frac{1}{fd_n} \tag{5}$$

In spite of the suspicion by Pletka and Wiederhorn [12] as noted above, we can easily show, from Equations 1 and 5, that the energy release rate and hence the Mode I stress intensity factor at the crack tip is independent of the crack length for double-torsion specimens [26].

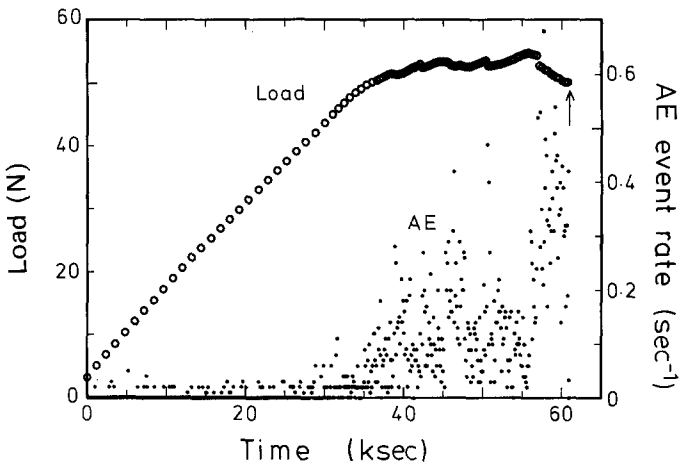

Figure 5 An example of the load–deformation curve and the event rate of acoustic emissions (AE) for Murata basalt under constant displacement rate. It shows a plateau region of the applied load, where the acoustic emission rate is also constant. An arrow indicates the macro-fracture of the plate. When the crack approaches the end of the plate, the stress intensity factor and hence the acoustic emission rates increase.

An example of the load–deformation curve observed in the constant displacement rate test is depicted in Fig. 5, where the event rate of the acoustic emissions is also shown. The crack velocity can be determined from the load of the plateau region in the figure. In this region, the acoustic emission rate as well as the applied load is constant, indicating that the crack velocity is constant and hence the stress intensity factor is also constant. When the macrocrack approaches the end of the plate, the load decreases and acoustic emissions increase. This is because of the increase in the stress intensity factor at the crack tip due to the interaction between the macrocrack and the end of the plate [26].

Figs 4 and 5 shows that the stress intensity factor is independent of the crack length for double-torsion specimens. Why can the hysteresis over several runs of the relaxation method be observed? Swanson [27] suggested that the time-dependent formation of the process zone and/or friction-induced locking between the crack surfaces are possible cause(s) of the hysteresis for polycrystalline materials.

Sano [16] showed that the stress corrosion index of Oshima granite should be around 30, using the constant load method of the double-torsion test. Indirect measurement of the index based on the influence of the strain rate on the uniaxial compressive strength of the same granite also showed that the stress corrosion index should be 32 [19, 28]. These conclusions agree well with the result of the fourth run shown in Fig. 3. However, in the relaxation tests, similar results as in the fourth run could be seen only when the initial load was sufficiently high and d_n was small enough. For Oshima granite, the critical width of d_n was around 1.6 mm, while the mean grain size of this granite is about 1 mm. Swanson [23, 27] found that the macrocrack frequently propagates along the grain boundaries when the crack velocity is relatively low. The probability of locking at the crack faces along grain boundaries may be high when d_n is somewhat larger than the mean grain size. This may explain why no hysteresis can be observed on soda-lime glass.

Fig. 6 shows the K–V diagram of Murata basalt obtained by using three different methods. Crosses and circles indicate the results of the relaxation method, squares indicate the constant displacement rate, and triangles denote the constant load. A bar on a square symbol shows the stress corrosion index determined from the load–deformation curve (for details see Section 4). Filled symbols indicate the crack velocity in water, which shows that the crack velocity in water is higher than in air by two or three orders of magnitude. This is experimental evidence showing that the water acts as a chemical agent in the stress corrosion processes of silicate materials [1–3].

Although hysteresis was observed in several experimental runs of the relaxation method, the data for this method where the above conditions are fulfilled agree well with the data from the constant load and the constant displacement rate methods. The stress corrosion index of Murata basalt is around 27, which agrees well with the data of Sano [16]. For Oshima

TABLE I Shear modulus of various materials estimated by compliance calibration; for comparison, shear moduli determined by other methods are also indicated.

Materials	Loading/unloading	Shear modulus (GPa)	
		Compliance	Other methods
Soda–lime glass	In either case	26.1 ± 0.4	27.3*
Murata basalt	Loading	26.8 ± 0.9	
	Unloading	27.4 ± 0.9	29.2 ± 0.5†
Quartz andesite	Loading	29.7 ± 1.0	
	Unloading	29.7 ± 1.0	27.2 ± 0.5†
Oshima granite	Loading	24.1 ± 3.5	
	Unloading	26.4 ± 3.5	23.8 ± 0.4†

*Dynamic modulus
†Modulus by uniaxial compression test.

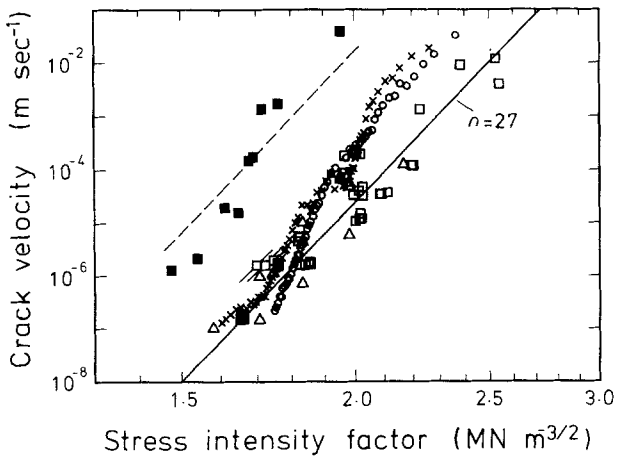

Figure 6 The sress intensity factor–crack velocity diagram of Murata basalt obtained by using three different methods of the double-torsion technique. (x, ○) Load-relaxation method; (□, ■) constant displacement rate method; (△) constant load method. Filled symbols indicate crack velocity in water.

granite, the K–V relation by the relaxation tests where the above conditions are satisfied is shown in Fig. 7 with the data of the constant displacement rate tests. These data also agree well with each other. The subcritical crack growth data shown in Figs 6 and 7 should therefore give the intrinsic material property, and the data indicating a high value of the stress corrosion index as shown in Fig. 3 may be brought about by some experimental disturbance. Because the relaxation method has the advantage that a wide range of data can be obtained from a single experimental run, many authors have usually employed this method. However, the hysteresis described above occasionally makes the data unreliable. The relaxation tests should be carried out in combination with one of the other methods in order to verify the experimental data.

Fig. 7 also shows the anisotropy of the crack velocity within Oshima granite. The crack velocity in the GR specimens (Fig. 7b) is much higher than the one in the GH specimens (Fig. 7a) by several orders of magnitudes at the same stress levels. GH indicates the same as in Fig. 3. GR indicates that the direction of crack opening is normal to the "rift" plane [20].

5. Discussion

The data from the constant displacement rate test of the double-torsion technique do not show any hysteresis in the K–V diagram. This method should be more reliable than the relaxation test. However, a single experimental run has been able to determine only one point in the K–V diagram. Thus many specimens and many experimental runs have been needed to determine the K–V relation of the material. This could be the main reason why the constant displacement rate test has rarely been carried out.

In the constant displacement rate test, the deformation of the plate, z, is expressed by

$$z = A_1 t \tag{6}$$

The subcritical crack growth rate, da/dt, can be given by [1–3]

$$\frac{da}{dt} = AK_I^n \tag{7}$$

Combining Equations 4 and 7, we have

$$\frac{da}{dt} = A_2 P^n \tag{8}$$

where $A_2 = A\{W_m [3(1 + \nu)/(Wd_n d^3)]^{1/2}\}^n$. Differentiating Equations 2 and 6 with respect to time and combining the results, we have

$$\frac{dP}{dt}(Ba + D) + PB\frac{da}{dt} = A_1 \tag{9}$$

Substituting Equation 8 into Equation 9, and considering $P(Ba + D) = A_1 t$, Equation 9 leads to

$$\left(\frac{A_1 t}{P}\right)\frac{dP}{dt} = A_1 - BA_2 P^{n+1}$$

or

$$\frac{dP}{P} + A_3 P^n \frac{dP}{1 - A_3 P^{n+1}} = \frac{dt}{t} \tag{10}$$

where $A_3 = BA_2/A_1$. Integrating Equation 10, we have

$$\log P - \frac{\log (1 - A_3 P^{n+1})}{n + 1} = \log (t) + C_1 \tag{11}$$

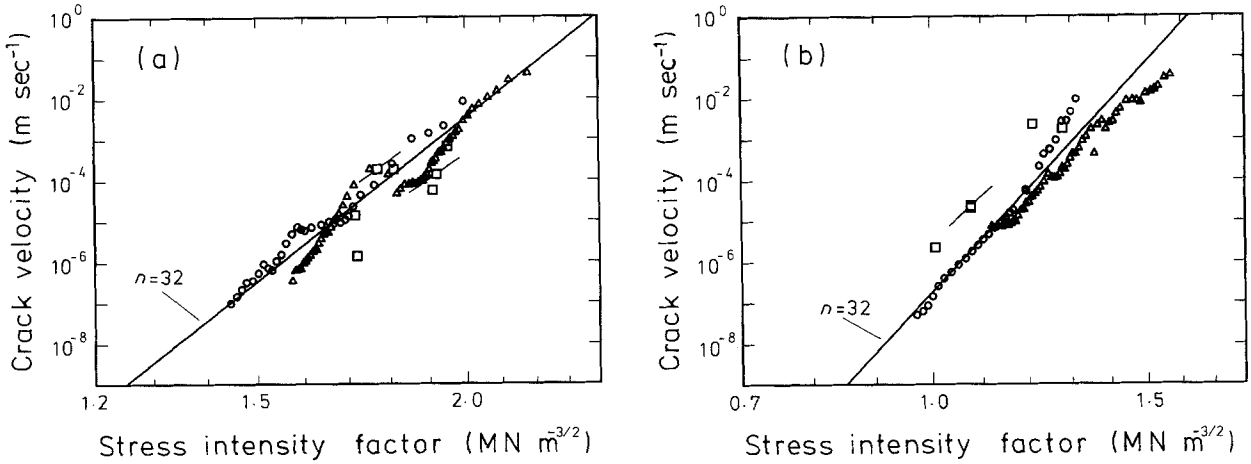

Figure 7 The stress intensity factor–crack velocity diagram of Oshima granite obtained by using two methods: (□) constant displacement rate and (○, △) load-relaxation method. (a) GH specimens and (b) GR specimens where G indicates that the crack propagates in the direction normal to the grain plane, and H and R indicate that the crack opens in the direction normal to the hardway plane and the rift plane respectively.

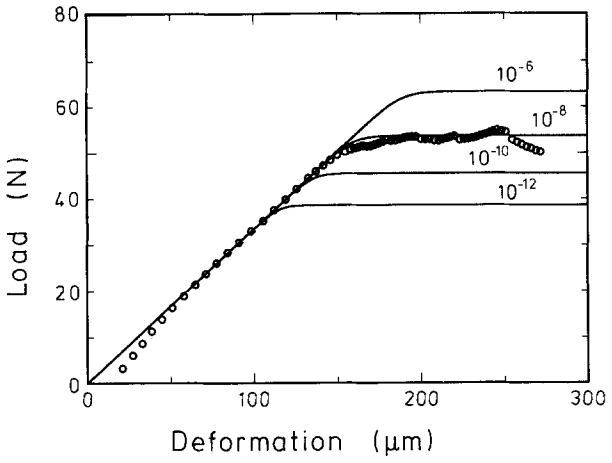

Figure 8 Theoretically calculated load–deformation curve of double torsion specimens under constant displacement rates of various values. The displacement rate is shown at each theoretical curve in m sec^{-1}. (O) Observed load–deformation curve of Murata basalt for comparison.

where C_1 is an integration constant. The load P is equal to P_1, when $t = 1$. Equation 11 yields

$$P(1 - A_3P^{n+1})^{-1/(n+1)} = \frac{zP_1}{A_1}(1 - A_3P_1^{n+1})^{-1/(n+1)}$$

or

$$z = \frac{A_1P}{P_1}\left(\frac{1 - A_3P_1^{n+1}}{1 - A_3P^{n+1}}\right)^{1/(n+1)} \quad (12)$$

When C_0 is the initial compliance, $A_1 = P_1C_0$ should hold. Then Equation 12 yields

$$z = PC_0\left(\frac{1 - A_3(A_1/C_0)^{n+1}}{1 - A_3P^{n+1}}\right)^{1/(n+1)} + z_0 \quad (13)$$

where z_0 is a constant depending on the non-linearity of the early stage of the load–deformation curve. The constant also involves the inelastic deformation of the plate produced in the previous loading cycles. Equation 13 expresses the load–deformation relation of the double-torsion specimens under constant displacement rate. Note that Equation 13 does not hold for the specimens without macrocracks. Before this equation is applied, pre-cracking is, therefore, inevitably needed.

When the loading system and the specimen are fixed, the variables in Equation 13 are A_1, A and n. The effect of the displacement rate, A_1, on the load–deformation curve is shown in Fig. 8. The maximum plateau region can be predicted theoretically. The higher the displacement rate, the higher the maximum load, as suggested by Evans [7]. One point in the K–V diagram can be determined by the plateau load. Furthermore, when the displacement rate is fixed, the variables are only A and n. As the K–V curve passes through the point determined by the maximum load, parameters A and n are dependent on each other. Now the stress corrosion index, n, is the only variable. Using Equation 13, theoretically calculated load–deformation curves are shown in Fig. 9 with the experimental load–deformation curve. The parameter n is also shown in the figure. In Fig. 9a, the stress corrosion index of soda–lime glass ranges from 10 to 20. This agrees well with the result from double-torsion experiments [7] and that obtained from double-cantilever-beam tests by Wiederhorn [29]. The stress corrosion index of both Murata basalt and Oshima granite ranges from 10 to 30, which is in harmony with the results described above. In principle, only one experimental run by the constant deformation rate method can, therefore, determine the full characteristics of subcritical crack growth in the material.

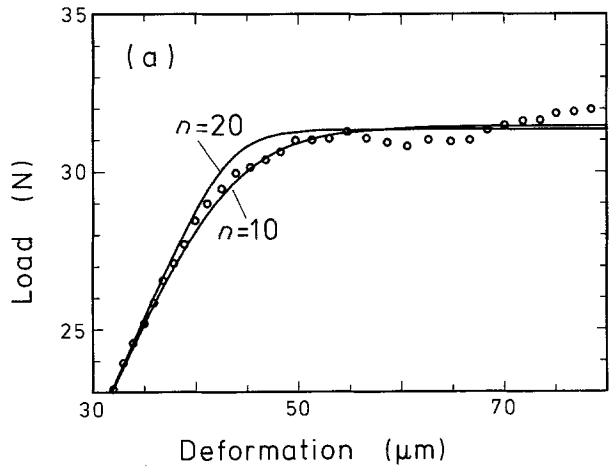

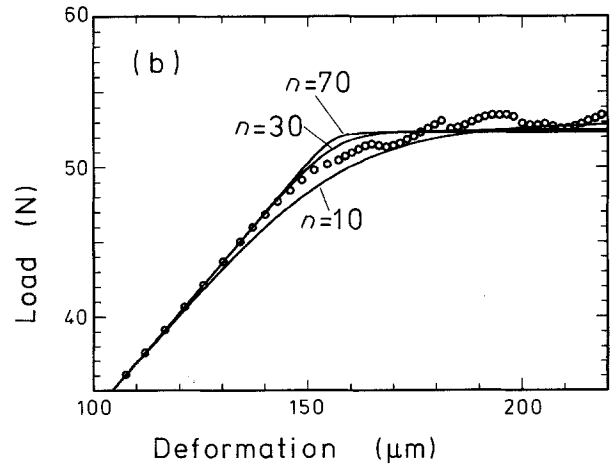

Figure 9 The stress corrosion index of the materials can be determined from the load–deformation curve under constant displacement rate. The index is estimated by comparing the observed load–deformation curve with the calculated ones. The subcritical crack growth data can be, in principle, determined by a single experimental run of the constant displacement rate test. (O) Experimental points for (a) soda–lime glass, (b) Murata basalt, (c) Oshima granite.

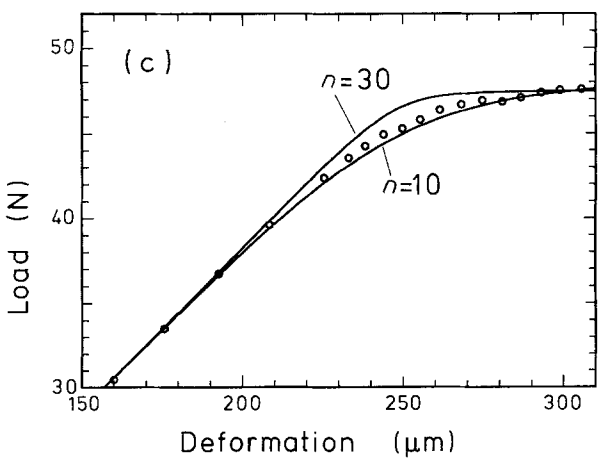

6. Conclusions

Relatively large scattering of the K–V relation was observed in several experimental runs of the load-relaxation method of double-torsion testing. This hysteresis in the K–V diagram can hardly be observed in the other two methods, the constant load and the constant displacement rate methods. In spite of doubts about the constant K, it was confirmed again that the stress intensity factor at the crack tip is independent of the crack length for double-torsion specimens.

Although the advantage of the relaxation method has been noticed, the hysteresis of the data obtained by this method makes the result unreliable. The relaxation experiment should be carried out in combination with other methods. A theoretical calculation of the load–deformation curve under constant displacement rate can, in principle, estimate the stress corrosion index. Then only one experimental run of this method can give a verification of the results from the load–relaxation method of double-torsion testing.

References

1. R. ADAMS and P. W. McMILLAN, *J. Mater. Sci.* **12** (1977) 643.
2. R. W. DAVIDGE, "Mechanical Behaviour of Ceramics" (Cambridge University Press, Cambridge, 1979) Ch. 9.
3. O. L. ANDERSON and P. C. GREW, *Rev. Geophys. Space. Phys.* **73** (1977) 1433.
4. B. R. LAWN and T. R. WILSHAW, "Fracture of Brittle Solids" (Cambridge University Press, Cambridge, 1975) Chs 3, 8.
5. J. O. OUTWATER and D. J. GERRY, *US Naval Research Laboratory Report* **NONR 3219** (1966).
6. J. A. KIES and A. B. J. CLARK, in "Fracture", edited by P. L. Pratt (Chapman and Hall, New York, 1969) p. 483.
7. A. G. EVANS, *J. Mater. Sci.* **7** (1972) 1137.
8. B. J. PLETKA, E. R. FULLER Jr and B. G. KOEPKE, **STP 678** (American Society for Testing and Materials, Philadelphia, 1979) p. 19.
9. B. K. ATKINSON, *Pure Appl. Geophys.* **117** (1979) 1011.
10. B. K. ATKINSON and P. G. MEREDITH, *Tectonophysics* **77** (1981) T1.
11. P. L. SWANSON, *J. Geophys. Res.* **89** (1984) 4137.
12. B. J. PLETKA and S. M. WIEDERHORN, in "Fracture Mechanics of Ceramics", Vol. 4, edited by R. C. Bradt, D. P. H. Hasselman and F. F. Lange (Plenum, New York, 1978) p. 745.
13. M. K. FERBER and S. D. BROWN, *J. Amer. Ceram. Soc.* **63** (1980) 424.
14. A. G. EVANS and S. M. WIEDERHORN, *J. Mater. Sci.* **9**(1974) 270.
15. T. WAZA, K. KURITA and H. MIZUTANI, *Tectonophysics* **67** (1980) 25.
16. O. SANO, *Int. J. Rock. Mech. Min. Sci. Geomech. Abstr.* **18** (1981) 259.
17. T. A. MICHALSKE, M. SINGH and V. D. FRECHETTE, **STP 745** (American Society for Testing and Materials, Philadelphia, 1981) p. 3.
18. L. S. COSTIN and J. J. MECHOLSKY, in Proceedings of 24th US Symposium on Rock Mechanics, Texas A & M University, College Station, June 1983, edited by E. R. Hoskins (Association of Engineering Geologists) p. 385.
19. O. SANO, I. ITO and M. TERADA, *J. Geophys. Res.* **86** (1981) 9299.
20. T. N. DALE, *Bull. US Geol. Surv.* **738** (1923) 1.
21. S. S. PENG and A. M. JOHNSON, *Int. J. Rock. Mech. Min. Sci.* **6** (1972) 37.
22. B. K. ATKINSON and R. D. RAWLINGS, in "Earthquake Prediction", edited by D. W. Simpson and P. G. Richards (American Geophysical Union, Washington, DC, 1981) p. 605.
23. P. L. SWANSON, MS Thesis, University of Colorado (1980).
24. D. P. WILLIAMS and A. G. EVANS, *J. Test. Eval.* **1** (1972) 264.
25. A. D. JAYATILAKA, "Fracture of Engineering Brittle Materials" (Applied Science, London, 1979) Ch. 6.
26. G. G. TRANTINA, *J. Amer. Ceram. Soc.* **60** (1977) 338.
27. P. L. SWANSON, "Subcritical Fracture Propagation in Rocks", PhD thesis, University of Colorado (1985).
28. O. SANO, M. TERADA and S. EHARA, *Tectonophysics* **84** (1982) 343.
29. S. M. WIEDERHORN, *J. Amer. Ceram. Soc.* **50** (1967) 407.

Received 17 July
and accepted 12 November 1987